

# Surface-Enhanced Raman Study of Cyanide Adsorption at the Platinum Surface

Bin Ren,<sup>\*,†</sup> De-Yin Wu,<sup>†</sup> Bing-Wei Mao,<sup>‡</sup> and Zhong-Qun Tian<sup>\*,‡</sup>

Department of Chemistry, State Key Laboratory for Physical Chemistry of Solid Surfaces, Xiamen University, Xiamen 361005, China

Received: March 21, 2002; In Final Form: January 23, 2003

A detailed surface Raman study of the effect of the bulk concentration of cyanide ( $\text{CN}^-$ ), electrode potential, and immersion potential on the adsorption behavior of  $\text{CN}^-$  on the Pt electrode surface was performed on a confocal microprobe Raman system. The notable change of the C–N frequency and the Pt–C intensity at ca.  $-0.7$  V (vs SCE) indicates a subtle change of the adsorption behavior of  $\text{CN}^-$  on the platinum electrode in solutions with concentration of about  $10^{-4}$  M or lower. The concentration of cyanide in the bulk solution affects the adsorption behavior. The surface Raman signal can still be observed at concentrations as low as  $10^{-6}$  M. When the  $\text{CN}^-$  concentration is higher than  $10^{-3}$  M, the potential for immersing the platinum electrode in the  $\text{CN}^-$  solution has a remarkable effect on the adsorption behavior of  $\text{CN}^-$ . With the high-quality surface Raman spectra, the surface enhancement factor for the adsorbed  $\text{CN}^-$  was estimated to be about 150.

## Introduction

Studies of cyanide ion ( $\text{CN}^-$ ) adsorption on metal surfaces are of great interest to electrochemists from both theoretical and experimental points of view.<sup>1</sup> As a specific adsorbate, the adsorption of cyanide ion on an electrode surface can provide a wider double layer region for the electrode due to the suppression of the hydrogen and oxygen evolution. Therefore it becomes easier to probe the potential-dependent dynamics of the interface in the absence of complications from electrode-mediated reactions, which will lead to a more thorough understanding of the nature of the electrode/solution interface.<sup>2</sup> Since  $\text{CN}^-$  is iso-electronic with carbon monoxide (CO), it presents an interesting comparative case for CO.<sup>2,3</sup> On the other hand, cyanide is a very important complex ion in the electroplating industry to improve the plating quality, but the mechanism remains unclear.<sup>4</sup> Furthermore, it has been found that  $\text{CN}^-$  is an intermediate during the oxidation process of amino acids (such as serine and alanine).<sup>5</sup> Therefore,  $\text{CN}^-$  has been studied extensively by conventional electrochemical methods.<sup>6,7</sup> However, it has been found that it can adsorb strongly in the whole potential region on most noble metal surfaces, therefore the electrochemical study cannot provide much information concerning the adsorption configuration. With the fast development of spectroelectrochemistry in the 1980s and thereafter,<sup>8</sup> researchers have been seeking help from spectroelectrochemistry to achieve more information.

There are a number of investigations using infrared (IR) and sum frequency generation (SFG) techniques to gain insight into the double layer features such as the molecular structure and the orientation of the adsorbate under equilibrium conditions. Compared to the case of adsorbed CO, there are only a few in-situ IR spectroscopic studies of the cyanide species on platinum electrodes in electrochemical systems for two reasons: on one hand, it is difficult to obtain useful information

from the spectral data that tend to be rather complex; on the other hand, there is a comparative small IR cross section of  $\text{CN}^-$  ion compared with CO, which makes it difficult to obtain high-quality spectra. Although various acquisition techniques have been developed to eliminate spectral interference of other species, Kunitatsu et al. and Ashley et al. pointed out that IR spectroscopic features of surface cyanide species on Pt and Ag electrodes are often obscured by the solution species near the interface, especially when solutions with very high  $\text{CN}^-$  concentration ( $>0.1$  M) were used.<sup>1,2,9–11</sup> The complex nature of the spectra adds further difficulties to the assignment of vibrational bands.<sup>1,2,12–14</sup> To eliminate the interference from solution species, a procedure to electrochemically dose  $\text{CN}^-$  onto platinum electrodes has been used for the study of the  $\text{CN}^-$  adsorption under ultrahigh-vacuum (UHV) conditions.<sup>3,15,16</sup> The interference of the solution species with the surface species present in IR spectroscopy can be overcome by sum frequency generation (SFG), a highly surface-specific technique.<sup>17–22</sup> However, it is still somewhat ambiguous to determine the adsorption behavior of  $\text{CN}^-$  only by the  $\nu_{\text{CN}}$  in the high-frequency region.

Contrary to the above cases, Raman spectroscopy provides spectral data over the full spectral width including the low-frequency region ( $<600\text{ cm}^{-1}$ ) reflecting the bonding between the adsorbate and substrate. Unfortunately, without any enhancement, the sensitivity of this technique for detecting monolayer surface species is extremely low. The discovery of surface-enhanced Raman scattering (SERS) effect in the 1970s has partially overcome this problem. However, the application of this technique has been restricted to Ag, Cu, and Au surfaces, which solely show giant surface enhancement effects.<sup>23–25</sup> There are some reports on  $\text{CN}^-$  adsorption on Ag, Cu, and Au surfaces;<sup>26–28</sup> however, there are none on the pure Pt surface, a very widely used electrode in electrochemistry. The large value of the imaginary part of its dielectric constant makes it unfavorable for creating giant SERS.<sup>29</sup> In a recent paper of Creighton, an ultrathin film of Pt was evaporated over the SERS active Ag film as the SERS substrate to investigate the SERS of  $\text{CN}^-$  on this bimetallic surface. However, the major bands

\* Authors to whom correspondence should be addressed. Tel: 86-592-2181906. Fax: 86-592-2085349. E-mail: bren@jingxian.xmu.edu.cn; zqtian@xmu.edu.cn.

<sup>†</sup> Department of Chemistry.

<sup>‡</sup> State Key Laboratory for Physical Chemistry of Solid Surfaces.

observed were from the surface complex and the interference from the Ag substrate became significant with the prolonged measurement time.<sup>30</sup> Recently, with the use of highly sensitive Raman instruments and special pretreatment procedures for different transition-metal surfaces, we are now able to extend SERS to chemical systems of broader interest, among them are pyridine, CO (pure CO and the CO produced by the dissociative adsorption of methanol), H, and  $\text{SCN}^-$  on Pt, pyridine, and pyrazine on Ni, and benzotriazole, thiourea, and pyridine on Fe, etc.<sup>31–37</sup> Although  $\text{CN}^-$  was found to be a weaker IR absorbent than CO, it is a stronger Raman scatterer. The success in obtaining a Raman signal of CO on Pt stimulated us to perform a Raman study of  $\text{CN}^-$  adsorption on Pt. In this paper, a surface Raman investigation of cyanide ion adsorption at a roughened massive Pt electrode surface was performed, with the main focus on the effect of the electrode potential, concentration of  $\text{CN}^-$ , and the immersion potential on the adsorption behavior. On the basis of the high-quality spectra, the surface enhancement factor of  $\text{CN}^-$  on Pt was estimated.

### Experimental Section

Raman measurements were performed on a confocal microprobe Raman system (LabRam I, Dilor).<sup>32</sup> It is a single spectrograph instrument equipped with a holographic notch filter and a CCD detector, and thus has a very high detection sensitivity. The size of the slit and pinhole were 200  $\mu\text{m}$  and 800  $\mu\text{m}$ , respectively. The 632.8 nm laser line from a He–Ne laser was used as the excitation line with a power of 8.5 mW on the sample. The microscope objective is a long-working distance one with 50 $\times$  magnification.

The electrode potential during Raman measurements was controlled by a PAR 173 potentiostat (EG&G). Cyclic voltammograms were recorded with a CHI631A electrochemical workstation (CH instruments, Inc.). The square-wave potential control for roughening was realized by the combination of the PAR 173 potentiostat and a GFG-8016G function generator (Good Will Instrument, Co. Ltd.).

The working electrode is a polycrystalline Pt rod embedded in a Teflon sheath with a geometric surface area of 0.1  $\text{cm}^2$ . The pretreatment and roughening procedure has been given elsewhere.<sup>32,37</sup> The real surface area of the Pt electrode used in this study is about 50 times larger than the ideally smooth polycrystalline Pt electrode of the same geometric area. The counter and reference electrodes are a large platinum ring and a saturated calomel electrode (SCE), respectively. All the chemicals used are of analytical grade and the solutions were prepared using Milli-Q water.

### Results and Discussion

**Electrochemical Study.** Figure 1 shows the cyclic voltammograms of a roughened Pt electrode in 0.1 M  $\text{KNO}_3$  solutions containing KCN with different concentrations. It can be seen from the curves that the characteristic hydrogen adsorption and desorption processes existing in the  $\text{KNO}_3$  solution were severely blocked by the strongly adsorbed  $\text{CN}^-$  when the concentration of KCN is higher than 0.1 mM. Moreover, the absence of a significant anodic current when the potential is more positive than +0.6 V and the cathodic current when the potential is more negative than –0.90 V indicates that the hydrogen evolution, the oxygen adsorption, and evolution processes were severely suppressed by the adsorption of  $\text{CN}^-$ . In the  $\text{KNO}_3$  solution, the surface oxidation of Pt occurs at about 0.6 V; however, in the solution containing 0.01 M KCN, a small and broad anodic peak appears at around 0.3 V, indicating that

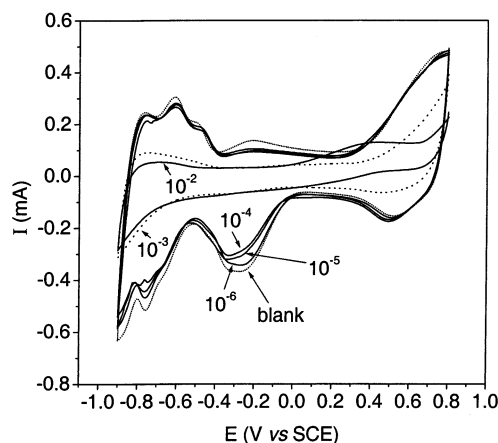


**Figure 1.** Cyclic voltammograms of a roughened Pt electrode in solutions with different concentrations of  $\text{CN}^-$ . The supporting electrolyte is 0.1 M  $\text{KNO}_3$  and the concentrations of KCN (M) are indicated in the figure. Scan rate: 50  $\text{mV s}^{-1}$ .

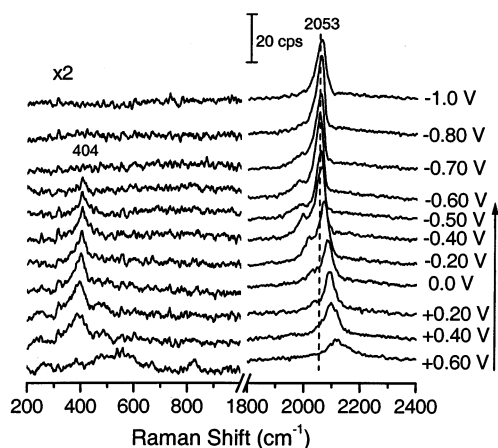


**Figure 2.** Potential-dependent surface-enhanced Raman spectra of  $\text{CN}^-$  adsorbed on a roughened Pt surface in a solution containing  $10^{-4}$  M KCN + 0.1 M  $\text{KNO}_3$ . Laser excitation line: 632.8 nm.

another oxidation process occurs in such a high-concentration solution. It could be due to the oxidation of Pt or the formation of a  $\text{CN}^-$  and Pt complex. It has been well documented that  $\text{CN}^-$  can adsorb very strongly at Pt electrodes over a wide potential range. Radiotracer experiments revealed that the surface coverage of  $\text{CN}^-$  keeps almost constant within the double layer and oxide regions and decreases significantly at the most positive potential, where  $\text{CN}^-$  is oxidized.<sup>2</sup> Our electrochemical result is similar to what has been reported. Unfortunately, besides this information, few additional details regarding the electrochemical or interfacial behavior of cyanide at the platinum surface can be obtained by conventional electrochemical techniques. Under this circumstance, the spectroscopic study of this system is highly desired to reveal the interfacial adsorption behavior of this ion at the molecular level.

**Potential Effect on the Cyanide Adsorption.** In previous studies, the electrode potential has been found to have a significant influence on the adsorption behavior of  $\text{CN}^-$  on Pt.<sup>1–22,26–28</sup> To this end, we performed a potential-dependent surface Raman study of  $\text{CN}^-$  on Pt. Figure 2 gives a series of potential-dependent Raman spectra (with selected potentials) from Pt in  $10^{-4}$  M KCN + 0.1 M  $\text{KNO}_3$  solution. The integrated intensities and vibrational frequencies of the bands at ca. 2100 and 400  $\text{cm}^{-1}$  as a function of the electrode potential were plotted and are given in Figure 3a and 3b, respectively. The two figures show several dramatic changes in the spectra upon

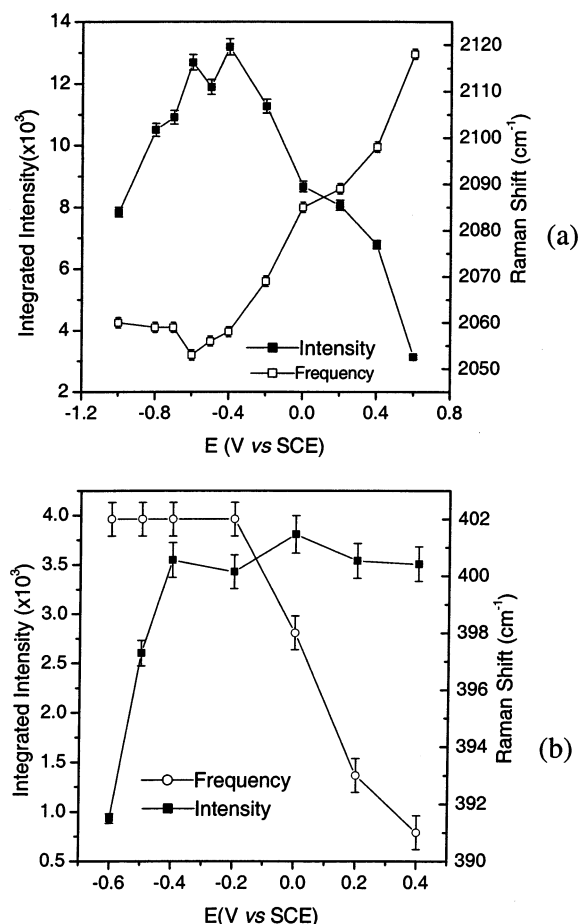


**Figure 3.** A plot of the integrated intensity, vibrational frequency for the bands at ca. 2100  $\text{cm}^{-1}$  (a) and 400  $\text{cm}^{-1}$  (b) changing with the electrode potential extracted from Figure 2.

negative movement of the electrode potential. (i) The band at about 2120  $\text{cm}^{-1}$  at 0.6 V, shifts to 2053  $\text{cm}^{-1}$  at -0.6 V and the intensity keeps growing. However, with further negative movement of the potential to -0.7 V, its frequency jumps back to 2059  $\text{cm}^{-1}$  and remains almost unchanged with the further negative movement of the potential while the intensity of the band decreases slightly. (ii) The intensity of the 400  $\text{cm}^{-1}$  band depends on the potential while its frequency blue-shifts only slightly. (iii) A new weak band appears in a narrow potential region from -0.2 to -0.6 V at ca. 1980  $\text{cm}^{-1}$  (see Figure 2, right side).

The most obvious change in the Raman spectra is the potential-induced frequency shift of the vibrational bands, which was considered to be due to the electrochemical Stark effect in the literature.<sup>38,39</sup> There are two main theories for interpreting this phenomenon: the potential-dependent metal and adsorbate chemical bonding and the influence of the variable electrostatic field. Although Lambert has pointed out that the two effects are equivalent in a complete description of the electronic polarization,<sup>38</sup> Weaver et al. found that the theoretically predicted  $d\nu_{\text{Pt-C}}/dE$  by the electrostatic field model is much smaller than that calculated from the experimental data, but the chemical bonding model gives a quite close approximation for the CO/Pt system.<sup>39</sup> Since  $\text{CN}^-$  is an iso-electronic molecule to CO, some of the description for the CO system can be borrowed for the interpretation of the  $\text{CN}^-$  system. As shown in ref 40, the  $\text{CN}^-$  adsorbed onto a  $\text{Pt}_{10(7,3)}$  cluster exhibits a charge transfer from  $\text{CN}^-$  to Pt, with only 0.43 e remaining on the CN. This is due to the large depopulation of the 5 $\sigma$  orbital,

the slight depopulation of the 4 $\sigma$  and 1 $\pi$  orbital, and the small population of the 2 $\pi$  orbital.<sup>40</sup> However, it was found that the 5 $\sigma$  orbital is only a weak antibonding orbital, the main influence on the change in the bond strength should originate from the depopulation of the strong antibonding 4 $\sigma$  orbital. The large frequency shift with the electrode potential (65  $\text{cm}^{-1} \text{V}^{-1}$ ) can be interpreted by the change in the extent of electron donation from the 4 $\sigma$  orbital of  $\text{CN}^-$  to the surface atoms of the Pt electrode. The change of the potential to a value more positive than the potential of zero charge (pzc, for a neutral solution the pzc of Pt is at around -0.2 to 0 V) results in an increasing depopulation of the strongly antibonding 4 $\sigma$  orbital of  $\text{CN}^-$ , thus strengthening the CN bond and leading to the blue-shift of the vibrational frequency. Contrarily, with a movement of the potential negative to the pzc, the CN bond is weakened and the frequency red-shifts. Actually, the electrostatic effect also gives a prediction of the same trend.<sup>38</sup> However, our spectral data obtained in the low-frequency region revealed that these two kinds of explanation are different.

It can be seen from Figure 2 that there is a band at ca. 400  $\text{cm}^{-1}$ , which can be assigned to the Pt-C stretching vibration. This assignment is supported by several experimental facts and theoretical prediction of Pt and  $\text{CN}^-$  complex<sup>41-43</sup> and the experimental data of the adsorbed CO on Pt surfaces.<sup>44-46</sup> The IR, Raman, and theoretical studies of Pt cyanide complexes show that the Pt-C band frequency is located in the region from 400 to 470  $\text{cm}^{-1}$ .<sup>42</sup> The MCSCF calculation of the Pt/ $\text{CN}^-$  system shows that the Pt-C frequency is at about 393  $\text{cm}^{-1}$ .<sup>43</sup> This value is surprisingly close to our data (396  $\text{cm}^{-1}$  at -0.2 V, around pzc). According to the electrostatic field effect, the Coulombic attraction between negatively charged  $\text{CN}^-$  ion (after adsorbing to a neutral Pt surface, CN still remains about 0.43 e charge)<sup>40</sup> and the surface should increase with the positive movement of the electrode potential. Therefore, the Pt-C frequency should also increase due to the strengthening of the Pt-C bond. However, our experimental data give an opposite trend with a stark effect value of -17  $\text{cm}^{-1} \text{V}^{-1}$ . This phenomenon can be interpreted by the chemical bonding effect: the positive movement of the electrode potential increases the donation of the electron from the 4 $\sigma$  orbital of  $\text{CN}^-$  to the 5d orbital of the metal, which strengthens the Pt-C bond. On the other hand, it also results in a decrease in the back-donation from metal to the antibonding 2 $\pi$ , which weakens the Pt-C band. The tradeoff between these two effects results in a relatively small stark effect. The dominant effect of the latter decreases the frequency of the Pt-C vibration. From the shifting trend of the Pt-C vibration we can draw a conclusion that, in the  $\text{CN}^-/\text{Pt}$  system, the chemical bonding effect dominates the electrochemical Stark effect.

It can be seen from Figure 2 that the CN band did not undergo the changes described by other authors in high-concentration situations.<sup>1-22</sup> In their experiments, they found a band at 2140  $\text{cm}^{-1}$  with a small Stark tuning value ( $d\nu_{\text{CN}}/dE$ , 10  $\text{cm}^{-1} \text{V}^{-1}$ ) at positive potentials ( $>0.2$  V) and a band with large  $d\nu_{\text{CN}}/dE$  (65  $\text{cm}^{-1} \text{V}^{-1}$ ) at negative potentials ( $<0.2$  V), which has been considered to be the characteristic of the on-top adsorbed N-bonded and C-bonded species, respectively.<sup>15-22,47-49</sup> However, some groups assign the band at 2140  $\text{cm}^{-1}$  to the surface complex, hydrocyanide,<sup>15,16</sup> or  $\text{CN}^-$  adsorbed on the disordered surface site.<sup>20-22</sup> In our experiment, only one trend was observed in the potential region more positive than -0.6 V with a large  $d\nu_{\text{CN}}/dE$  value. The species was assumed to bind to the surface with the C end as supported by the only one low-frequency band appearing at ca. 400  $\text{cm}^{-1}$  with a negative  $d\nu_{\text{Pt-CN}}/dE$



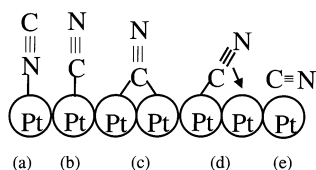


**Figure 4.** Five proposed adsorption models of  $\text{CN}^-$  adsorbed on metal surfaces: (a) C-end linearly adsorbed; (b) N-end linearly adsorbed; (c) bridge bonded; (d) semi-bridge bonded; (e) flat bonded.

value. This finding demonstrates that the concentration of cyanide should have an effect on the adsorption behavior of  $\text{CN}^-$  on the surface and raises a question that if the appearance of  $2140\text{ cm}^{-1}$  band is from the C-end species and depends only on the electrode potential, the present experiment should be able to detect it.

Besides the change in frequency, the Raman intensity of the  $\nu_{\text{CN}}$  increases when the electrode potential was moved from  $+0.6$  to  $-0.4\text{ V}$ . It cannot be simply interpreted by the increase of the surface coverage since the electrode potential at the maximum intensity is much more negative than the pzc although  $\text{CN}^-$  is a specifically adsorbed anion. Actually, conventional electrochemical investigations revealed that  $\text{CN}^-$  can adsorb on the Pt surface in the whole double layer region.<sup>7</sup> At present we cannot rule out the possible contribution of the charge-transfer effect, which will lead to the appearance of a maximum on the intensity–potential curve.<sup>50</sup> However, the verification of this assumption meets an obstacle since the  $\nu_{\text{CN}}$  experiences a sudden frequency change after the peak intensity reaches the maximum with the negative movement of the electrode potential. This reveals that the Raman band observed at potentials more negative or positive than  $-0.7\text{ V}$  is from the  $\text{CN}^-$  species in a different configuration. After considering the sudden change in the frequency (this phenomenon has been verified by experiments with different laser excitations, different  $\text{CN}^-$  concentrations lower than  $0.1\text{ mM}$ , and different immersion potentials), we think a possible reason for the intensity and frequency change could be the orientation change of the adsorbed  $\text{CN}^-$  on the Pt surface.

In the literature, at least five kinds of adsorption configuration for  $\text{CN}^-$  on various metal surfaces have been proposed, the models of which are shown in Figure 4: (a) and (b) the on-top adsorbed  $\text{CN}^-$  with either the N or C end to the surface; (c) bridge-type adsorbed  $\text{CN}^-$  with its C end adsorbed onto two Pt atoms;<sup>10</sup> (d) the semi-bridge type with its C end forming a  $\sigma$  bond with a Pt atom and its  $\pi$  bond binding to the Pt surface;<sup>15</sup> and (e) the  $\text{CN}^-$  lying flat on the Pt surface with its molecular axis parallel to the electrode surface and interacting with Pt through its  $\pi$  bond.<sup>51</sup> In electrochemical environments, the former four types of adsorption configurations have all been reported, and the last one has been found only at the gas/solid interface on the Cu(111) and Pd(100) and (111) surfaces.<sup>51</sup> In the literature, there are still some controversies on the charge distribution in the  $\text{CN}^-$  ion.<sup>43,52</sup> Our recent calculation by using HF and B3LYP methods with different basis sets revealed that the C end is negatively charged, but slightly more positive than the N end.<sup>53</sup> However, due to the strong coordination effect of the C atom with Pt,  $\text{CN}^-$  prefers to adsorb with its C-end to the Pt surface even at potentials more positive than pzc, see Figure 4b. This assignment is supported by the  $\nu_{\text{Pt-C}}$  band appearing in the potential range more positive than  $-0.6\text{ V}$ . With the negative movement of the potential, the C-end species at some sites may prefer to sit in the bridge site, see Figure 4c, especially when the surface coverage of  $\text{CN}^-$  is low, as in the case of CO.<sup>44–46</sup> This assumption is supported by the appearance

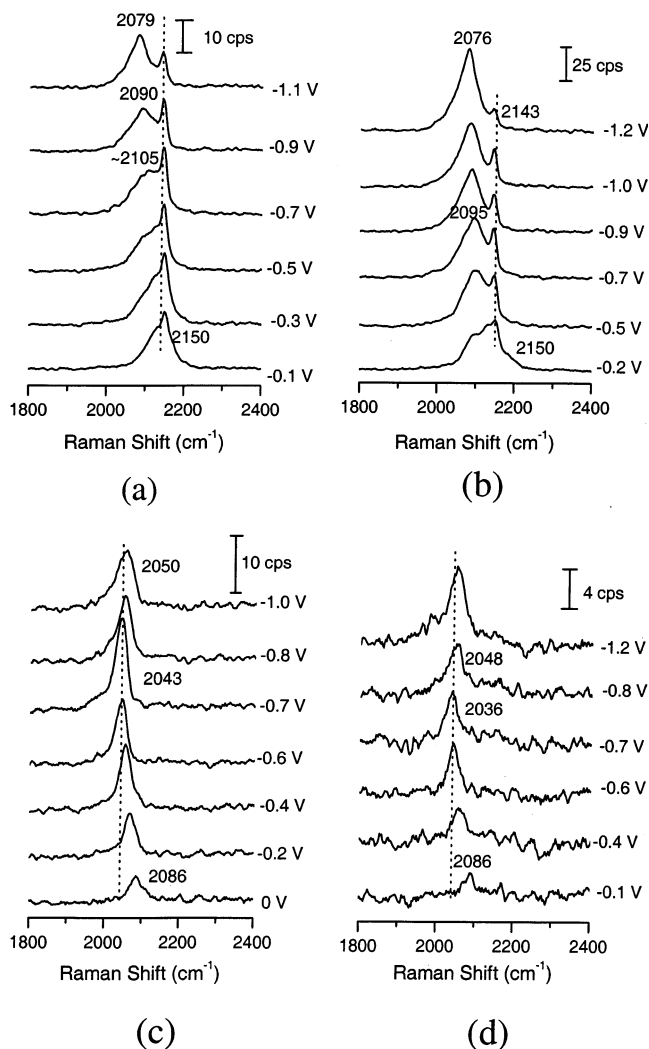


**Figure 5.** Surface-enhanced Raman spectra from a roughened Pt electrode in  $0.1\text{ M KNO}_3$  solutions with different  $\text{KCN}$  concentration: (a)  $10^{-2}\text{ M}$ ; (b)  $10^{-3}\text{ M}$ ; (c)  $10^{-5}\text{ M}$ ; (d)  $10^{-6}\text{ M}$ . Laser excitation line:  $632.8\text{ nm}$ .

of the band at  $1980\text{ cm}^{-1}$ , which have been assigned to the bridge-bonded  $\text{CN}$  on the Pt surface by Takamaru et al.<sup>54</sup> and Ashley et al.<sup>1</sup> When the potential shifts further negative to  $-0.7\text{ V}$ , a sudden change in the frequency of  $\text{CN}^-$  was found. Meanwhile, the Pt–C band cannot be detected any more. This indicates a subtle change in the adsorption mode of  $\text{CN}^-$  on the surface. More interestingly, the  $\text{CN}^-$  frequency almost does not shift with potential. This species can be tentatively assigned to the flatly adsorbed species, see Figure 4e. We have no evidence for the existence of the  $\sigma + \pi$  species as proposed by Korzeniewski et al.<sup>15</sup> However, if it exists, it may appear in the potential region from  $-0.6$  to  $-0.7\text{ V}$ , when the adsorption mode of  $\text{CN}^-$  ion changes from the on-top one to the flat one.

Our results are at variance to what has been published heretofore. The differences in experimental condition, especially the concentration of  $\text{CN}^-$ , may account for this. In the studies of Tadjeddine,<sup>17–19</sup> Ito,<sup>12</sup> Daum,<sup>20–22</sup> Aldaz,<sup>5,13,49</sup> Ashley,<sup>1,2,9,10</sup> and Zhang,<sup>14</sup> solutions containing high  $\text{CN}^-$  concentration were used ( $1\text{ mM}$  to  $0.1\text{ M}$ ), and in the studies of Cooney,<sup>3</sup> Korzeniewski,<sup>15,16</sup> and Stuhlmann,<sup>47,48</sup> a preadsorption method was adapted (either in the solution or in the UHV chamber) previous to experiments. The initial  $\text{CN}^-$  concentrations in the bulk solution used to form adsorbed  $\text{CN}^-$  in their experiment is higher than that of ours ( $10^{-4}\text{ M}$ ). Therefore, we performed

a concentration-dependent study in order to achieve a better understanding of the difference.

**Concentration-Dependent Adsorption Behavior of Cyanide.** The  $\text{CN}^-$  concentration used in this study ranges from 0.01 M to  $10^{-6}$  M. The surface Raman spectra were shown in Figures 2 and 5 for selected potentials. It can be seen from the figures that two overlapping bands are found at concentrations higher than 1 mM. The frequency of the low-frequency band shifts dramatically with the potential, while the band at  $2140\text{ cm}^{-1}$  shows a very small electrochemical Stark tuning rate. The latter gives lower intensity in 1 mM KCN solution than in 10 mM solution. Furthermore, this band is very hard to remove even when the electrode is controlled at very negative potentials. This behavior, together with the sharp band shape, allows us to assign it to the vibration of surface complex of Pt and  $\text{CN}^-$ , possibly  $\text{Pt}(\text{CN})_2^{2-}$ .<sup>15,21</sup> Further evidence comes from some IR studies, in which the surface complex was detected in the solution when the Pt electrode was held at a relative positive potential. It is reasonable that with the increase in the  $\text{CN}^-$  concentration near the electrode surface,  $\text{CN}^-$  can easily form surface complexes with Pt, which is favorable especially when the electrode is immersed into the solution without potential control (at open circuit potential). At lower concentrations, due to the lack of sufficient  $\text{CN}^-$  near the surface, the formation of the surface complex cannot be accomplished. This is supported by the decrease or even diminution of the intensity of this Raman band when the concentration is lower than  $10^{-3}$  M.

Another impressive phenomenon in this concentration-dependent Raman study is the remarkable frequency decrease of the CN stretch vibration upon the lowering of the solution  $\text{CN}^-$  concentration. A similar phenomenon has already been observed in the study of the CO coverage effect on the vibrational frequency of CO adsorbed on Pt-group metals and it was found that the dipole-dipole coupling among the adsorbed CO will lead to an increase in the vibrational frequency of CO.<sup>55</sup> One can find from Figure 5 that a large change of the band frequency occurs when the concentration changes from 1 mM to 0.1 mM. The frequency of the band shifts from ca. 2105, 2095, 2055, 2043 to  $2036\text{ cm}^{-1}$  when the concentration is decreased from  $10^{-2}$  to  $10^{-3}$ ,  $10^{-4}$ ,  $10^{-5}$ , and  $10^{-6}$  M (at  $-0.7\text{ V}$ ). The intensity for this band almost remains constant when the solution concentration is higher than  $10^{-3}$  M, which leads us to assume that  $\text{CN}^-$  could adsorb on the Pt surface saturatedly in this concentration range. This is also why there is no significant change in the vibrational frequency of  $\text{CN}^-$  with the solution concentration in this range. However, when the solution concentration is about  $10^{-4}$  M or lower, the  $\text{CN}^-$  ions near the surface are not sufficient to form a compact adsorbed  $\text{CN}^-$  layer resulting in a substantial decrease in the frequency. A further lowering in the surface coverage will not influence effectively the frequency because the separations among  $\text{CN}^-$  molecules are sufficiently large. This conclusion is supported by the minor decrease of the vibrational frequency of  $\text{CN}^-$  for concentrations lower than  $10^{-4}$  M at the same potential ( $-0.7\text{ V}$ ). Similar results were reported for  $\text{CN}^-/\text{Au}$  system by Kunimatsu, however, in a narrower concentration range.<sup>56</sup>

**The Immersion Potential Effect.** Most interestingly, we found that the immersion potential has a remarkable effect on the surface Raman spectra when the  $\text{CN}^-$  concentration is higher than 0.1 mM. Figure 6 gives two sets of Raman spectra from Pt in 0.01 M KCN solution obtained by immersing the electrode at different potentials. These spectra present very different surface Raman features at the same potential, which indicates that there exist different  $\text{CN}^-$  configurations on the surface. If

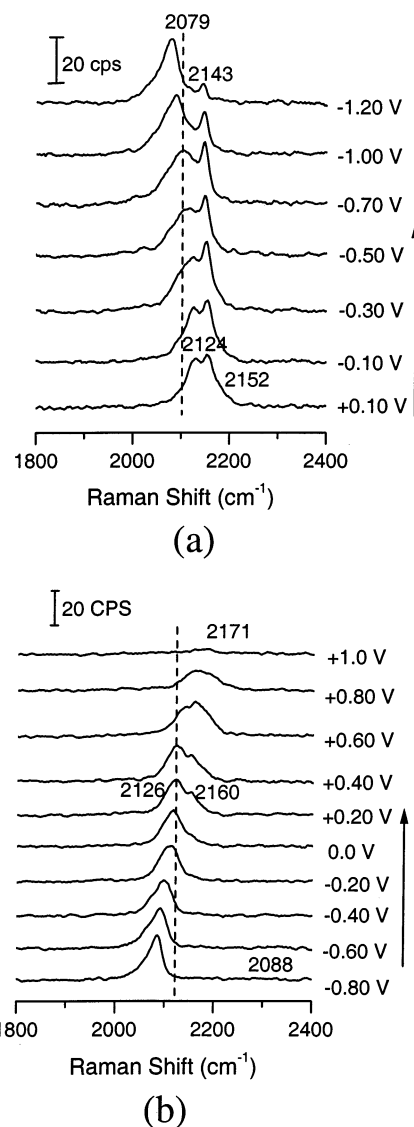


**Figure 6.** Surface-enhanced Raman spectra from a roughened Pt electrode in 0.1 M KCN + 0.1 M  $\text{KNO}_3$  solution. The electrode was immersed in the solution: (a) at  $-1.25\text{ V}$ , and (b) without potential control (at open circuit potential, ca.  $0.2\text{ V}$ ). Laser excitation line:  $632.8\text{ nm}$ .

the electrode was immersed without potential control, two bands coexist in the whole potential range. The band at ca.  $2100\text{ cm}^{-1}$  could be assigned to the  $\text{CN}^-$  species bonding through the C end, and that at  $2140\text{ cm}^{-1}$  to the surface cyanide complex. This phenomenon verifies our assumption in the previous section that  $\text{CN}^-$  can easily form a surface complex with Pt in the high  $\text{CN}^-$  concentration solution at the open circuit potential. It should be noted that the formation of a surface complex is irreversible, which is very difficult to remove even at a very negative potential (e.g.,  $-1.2\text{ V}$ ), see Figure 6a. Its intensity decreases slowly with an increase in the intensity of the adsorbed cyanide, indicating the transformation of the surface complex to the adsorbed surface species. On the other hand, when the electrode was immersed at  $-1.2\text{ V}$  only one Raman band could be detected in the whole potential range with the positive movement of the electrode potential, see Figure 6b. This species can be assigned to the C-end  $\text{CN}^-$ . The linear shift of the vibrational frequency with the electrode potential before the oxidation potential indicates that only one species exists at the surface before the oxidation of  $\text{CN}^-$ . In this aspect, our

assignment is different from the assumption of Tadjeddine<sup>19</sup> and Aldaz.<sup>13</sup> The band appearing at 2160–2171 cm<sup>-1</sup> is possibly from the oxidation product, OCN<sup>-</sup>.<sup>3,9–16</sup> The formation of a compact adlayer of CN<sup>-</sup> deactivates the Pt electrode and makes CN<sup>-</sup> difficult to oxidize until very positive potentials. This study clearly shows that the immersion potential has a significant effect on the adsorption of CN<sup>-</sup> on the Pt surface, and further demonstrates our previous assignment that the 2140 cm<sup>-1</sup> band is from the surface complex. No immersion potential effect could be observed when the concentration is lower than 10<sup>-3</sup> M.

**Calculation of the Surface Enhancement Factor for CN<sup>-</sup> at the Pt Surface.** After obtaining the surface Raman spectra of CN<sup>-</sup> on Pt, one may immediately ask whether there is SERS effect on this system. The surface enhancement factor ( $G$ ) can be calculated by comparing the Raman signal from the surface and the solution after considering the molecules effectively excited by the laser within the laser beam in the two situations. On the basis of the special feature of the confocal system, a method to calculate the surface enhancement factor was developed in our lab by the following equation:<sup>57</sup>

$$G = \frac{hcN_A\sigma I_{\text{surf}}}{RI_{\text{bulk}}} \quad (1)$$

where  $h$  is a characteristic value of the confocal Raman system and is determined by the setting of the confocal system<sup>57</sup> and in this experiment it is about 60  $\mu\text{m}$ .  $c$ ,  $N_A$ ,  $\sigma$ , and  $R$  are the concentration of CN<sup>-</sup>, the Avogadro constant, the surface area occupied by each CN<sup>-</sup> ion, and the roughness factor of the Pt electrode, respectively.  $I_{\text{surf}}$  and  $I_{\text{bulk}}$  are the integrated intensities of the surface Raman signal of the adsorbed CN<sup>-</sup> and the normal Raman signal of free CN<sup>-</sup> in solution, respectively. In this equation, the  $h$ ,  $c$ ,  $R$ ,  $I_{\text{surf}}$ , and  $I_{\text{bulk}}$  can be obtained through experiment.  $\sigma$  is the only unknown value and can be estimated by the following method. Expecting an extreme condition that one cyanide ion occupies one surface Pt atom, the maximum area occupied by one cyanide ion amounts to that of a unit cell of the Pt(111) surface. The area of a unit cell of a Pt(111) surface is about 0.0585 nm<sup>2</sup> as known from the bulk lattice constant of Pt. The STM study of CN<sup>-</sup> adsorption on a Pt surface showed that the CN<sup>-</sup> ions occupy only ca. 67% of the Pt(111) surface.<sup>48</sup> Taking this factor into account, a CN<sup>-</sup> occupies a surface area of 0.0878 nm<sup>2</sup>. The surface spectrum acquired in the KCN solution with the concentration of 1 mM was selected to calculate the surface enhancement factor because it gives the strongest signal of the adsorbed CN<sup>-</sup>. The surface Raman signal amounts to 1800 cps. For a better signal-to-noise ratio, the solution spectrum was acquired in a 0.1 M KCN solution, and the integrated intensity is about 90 cps. The Raman spectra for the surface species and solution species were given in Figure 7. With the known constant  $N_A = 6.02 \times 10^{23}$ , the surface enhancement factor is calculated to be 100 to 150, which is very close to that of pyridine adsorption on a platinum surface. This clearly shows the involvement of the enhanced Raman effect on this system.

## Conclusion

Using a highly sensitive confocal microprobe Raman system combined with the special roughening method for Pt, we are able to obtain surface Raman spectra of CN<sup>-</sup> adsorption on a pure Pt electrode surface, especially the molecule–metal vibration reflecting the adsorbate and substrate bonding. CN<sup>-</sup> ion was found to exist on the Pt surface in the whole potential range. In the potential-dependent study of the CN<sup>-</sup> adsorption

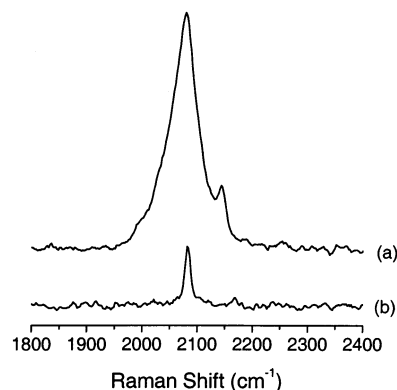


**Figure 7.** Surface Raman spectra of adsorbed CN<sup>-</sup> on a roughened Pt surface obtained in 10<sup>-3</sup> M KCN + 0.1 M KNO<sub>3</sub> solution at -1.2 V and the solution Raman spectrum obtained in 0.1 M KCN solution. Laser excitation line: 632.8 nm.

in the solution with a concentration of 10<sup>-4</sup> M, we found that CN<sup>-</sup> adsorbs to the Pt surface through its C end at relatively positive potentials, supported by the Pt–C band detected in the potential region more positive than -0.6 V. When the potential was made more negative, an orientation change is evident by the sudden change of the CN<sup>-</sup> stretching frequency and the disappearance of the Pt–C band, which leads us to assign this species to the flat adsorbed CN<sup>-</sup>. By analyzing the potential-dependent band frequency shift, we found that the chemical bonding effect accounts mostly for this phenomenon. In a concentration-dependent study, the surface coverage was found to affect significantly the vibrational frequency of the adsorbed CN<sup>-</sup> as a result of the dipole–dipole coupling between the adsorbed negatively charged CN<sup>-</sup> ion. Both the immersion potential-dependent and concentration-dependent studies revealed that the band at 2140 cm<sup>-1</sup> was due to the surface complex of CN<sup>-</sup> and Pt, possibly Pt(CN)<sub>2</sub><sup>2-</sup>, which exists in solutions of high CN<sup>-</sup> concentration and at relatively positive potentials, rather than the C-end adsorbed species. Further studies, including the isotopic effect, and a differential capacitance study will be of help for present study.

**Acknowledgment.** This work was supported by the Natural Science Foundation of China under contract numbers 29903009, 20021002, and 90206039.

## References and Notes

- (1) Ashley, K.; Lazaga, M.; Samant, M. G.; Seki, H.; Philpott, M. R. *Surf. Sci.* **1989**, 219, L590.
- (2) Ashley, K.; Weinert, F.; Samant, M. G.; Seki, H.; Philpott, M. R. *J. Phys. Chem.* **1991**, 95, 7409.
- (3) Hinman, A. S.; Kydd, R. A.; Cooney, R. P. *J. Chem. Soc., Faraday Trans.* **1986**, 82, 3525.
- (4) Reents, B.; Lacconi, G.; Plieth, W. *J. Electroanal. Chem.* **1994**, 376, 185.
- (5) Huerta, F.; Morallon, E.; Cases, F.; Rodes, A.; Vazquez, J. L.; Aldaz, A. *J. Electroanal. Chem.* **1997**, 431, 269.
- (6) Tamura, H.; Arikado, T.; Yoneyama, H.; Matsuda, Y. *Electrochim. Acta* **1974**, 19, 273.
- (7) Wieckowski, A.; Szklarczyk, M. *J. Electroanal. Chem.* **1982**, 142, 157.
- (8) *Spectroelectrochemistry—Theory and Practice*; Gale, R. J., Ed.; Plenum Press: New York, 1988.
- (9) Ashley, K.; Feldheim, D. L.; Parry, D. B.; Samant, M. G.; Philpott, M. R. *J. Electroanal. Chem.* **1994**, 373, 201.
- (10) Ashley, K.; Weinert, F.; Feldheim, D. L. *Electrochim. Acta* **1991**, 36, 1863.
- (11) Kunimatsu, K.; Seki, H.; Golden, W. G. *Chem. Phys. Lett.* **1984**, 108, 195.
- (12) Kitamura, F.; Takahashi, M.; Ito, M. *Chem. Phys. Lett.* **1986**, 130, 181.

- (13) Huerta, F. J.; Morallon, E.; Vazquez, J. L.; Aldaz, A. *Surf. Sci.* **1998**, 396, 400.
- (14) Zhang, J. J.; Lu, J. T.; Cha, C. X.; Feng, Z. G. *Acta Phys.-Chim. Sin.* **1989**, 5, 409.
- (15) Kim, C. S.; Korzeniewski, C. *J. Phys. Chem.* **1993**, 97, 9784.
- (16) Paulissen, V. B.; Korzeniewski, C. *J. Phys. Chem.* **1992**, 96, 4563.
- (17) Guyot-Sionnest, P.; Tadjeddine, A. *Chem. Phys. Lett.* **1990**, 172, 341.
- (18) Tadjeddine, A.; Guyot-Sionnest, P. *Electrochim. Acta* **1991**, 36, 1849.
- (19) Tadjeddine, A.; Peremans, A.; Lerille, A.; Zheng, W. Q.; Tadjeddine, M.; Flament, J. P. *J. Chem. Soc., Faraday Trans.* **1996**, 92, 3823.
- (20) Daum, W.; Friedrich, K. A.; Klunker, C.; Knabben, D.; Stimming, U.; Ibach, H. *Appl. Phys. A* **1994**, 59, 553.
- (21) Friedrich, K. A.; Daum, W.; Klunker, C.; Knabben, D.; Stimming, U.; Ibach, H. *Surf. Sci.* **1995**, 335, 315.
- (22) Daum, W.; Dederichs, F.; Muller, J. E. *Phys. Rev. Lett.* **1998**, 80, 766.
- (23) Otto, A.; Mrozek, I.; Grabhorn, H.; Akemann, W. *J. Phys. Condens. Matter* **1992**, 4, 1143.
- (24) Moskovits, M. *Rev. Mod. Phys.* **1985**, 57, 783.
- (25) Pettinger, B. In *Adsorption of Molecules at Metal Electrodes*; Lipkowski, J., Ross, P. N., Eds.; VCH: New York, 1992; Chapter 6.
- (26) Laufer, G.; Huneke, J. T.; Schaaf, T. F. *Chem. Phys. Lett.* **1981**, 82, 571.
- (27) Billman, J.; Otto, A. *Surf. Sci.* **1984**, 138, 1.
- (28) Wetzel, H.; Gerischer, H.; Pettinger, B. *Chem. Phys. Lett.* **1981**, 80, 159.
- (29) Cline, M. P.; Barber, P. W.; Chang, R. K. *J. Opt. Soc. Am. B* **1986**, 3, 15.
- (30) Hesse, E.; Creighton, J. A. *Chem. Phys. Lett.* **1999**, 303, 101.
- (31) Tian, Z. Q.; Gao, J. S.; Li, X. Q.; Ren, B.; Huang, Q. J.; Cai, W. B.; Liu, F. M.; Mao, B. W. *J. Raman Spectrosc.* **1998**, 29, 703.
- (32) Tian, Z. Q.; Ren, B.; Mao, B. W. *J. Phys. Chem. B* **1997**, 101, 1338.
- (33) Ren, B.; Xu, X.; Li, X. Q.; Cai, W. B.; Tian, Z. Q. *Surf. Sci.* **1999**, 427/428, 156.
- (34) Huang, Q. J.; Li, X. Q.; Yao, J. L.; Ren, B.; Cai, W. B.; Gao, J. S.; Mao, B. W.; Tian, Z. Q. *Surf. Sci.* **1999**, 427/428, 162.
- (35) Tian, Z. Q.; Ren, B.; Chen, Y. X.; Zou, S.; Mao, B. W. *J. Chem. Soc., Faraday Trans.* **1996**, 92, 3829.
- (36) Huang, Q. J.; Yao, J. L.; Mao, B. W.; Gu, R. A.; Tian, Z. Q. *Chem. Phys. Lett.* **1997**, 271, 101.
- (37) Ren, B.; Lin, X. F.; Jiang, Y. X.; Cao, P. G.; Xie, Y.; Huang, Q. J.; Tian, Z. Q. *Appl. Spectrosc.* **2003**, 57, 419.
- (38) Lambert, D. K. *Electrochim. Acta* **1996**, 41, 623.
- (39) Zou, S.; Weaver, M. J. *J. Phys. Chem.* **1996**, 100, 4237.
- (40) Ample, F.; Curulla, D.; Fuster, F.; Clotet, A.; Ricart, J. M. *Surf. Sci.* **2002**, 497, 139.
- (41) Nakamoto, K. *Infrared and Raman Spectra of Inorganic and Coordination Compounds*; John Wiley: New York, 1978.
- (42) Kubas, G. J.; Jones, L. H. *Inorg. Chem.* **1974**, 13, 2816.
- (43) Tadjeddine, M.; Flament, J. P. *Chem. Phys.* **1999**, 240, 39.
- (44) Zhang, Y.; Weaver, M. J. *Langmuir* **1993**, 9, 1397.
- (45) Chesters, M. A.; McDougall, G. S.; Pemble, M. E.; Sheppard, N. *Surf. Sci.* **1985**, 164, 425.
- (46) Anderson, A. B. *J. Electroanal. Chem.* **1990**, 280, 37.
- (47) Stuhlmann, C. *Surf. Sci.* **1995**, 335, 221.
- (48) Stuhlmann, C.; Villegas, I.; Weaver, M. J. *Chem. Phys. Lett.* **1994**, 219, 319.
- (49) Huerta, F.; Morallon, E.; Quijada, C.; Vazquez, J. L.; Aldaz, A. *Electrochim. Acta* **1998**, 44, 943.
- (50) Otto, A. In *Light Scattering in Solid*; Cardona, M., Guntherodt, G., Eds.; Springer-Verlag: Berlin, 1984; Vol. 4, p 289.
- (51) Kordesch, M. E.; Lindner, T.; Somers, J.; Stenzel, W.; Conrad, H.; Bradshaw, A. M.; Williams, G. P. *Spectrochim. Acta* **1987**, 43A, 1561.
- (b) Kordesch, M. E.; Stenzel, W.; Conrad, H. *Surf. Sci.* **1987**, 186, 601.
- (c) Kordesch, M. E.; Stenzel, W.; Conrad, H.; Weaver, M. J. *J. Am. Chem. Soc.* **1987**, 109, 1878.
- (52) Botschwina, P. *Chem. Phys. Lett.* **1985**, 114, 58.
- (53) Wu, D. Y.; Ren, B.; Tian, Z. Q. Unpublished data.
- (54) Kawashima, H.; Ikezawa, Y.; Takamura, T. *J. Electroanal. Chem.* **1991**, 317, 257.
- (55) Hollins, P.; Pritchard, J. *Prog. Surf. Sci.* **1985**, 19, 275.
- (56) Kunitatsu, K.; Seki, H.; Golden, W. G.; Gorden, J. G. II; Philpott, M. R. *Langmuir* **1988**, 4, 337.
- (57) Cai, W. B.; Ren, B.; Liu, F. M.; Li, X. Q.; She, C. X.; Cai, X. W.; Tian, Z. Q. *Surf. Sci.* **1998**, 406, 9.